Fractional Surface Doping by Topological Neutral Wall Intersections on Ge(111)

G. Ballabio,[1,2] A. Goldoni,[3] S. Modesti,[4,5] and E. Tosatti[1,2,6]

[1]*International School for Advanced Studies (SISSA), via Beirut 2-4, 34014, Trieste, Italy*
[2]*Istituto Nazionale per la Fisica della Materia, Unità SISSA, via Beirut 2-4, 34014, Trieste, Italy*
[3]*Sincrotrone Trieste S.C.p.A., S.S. 14 Km 163.5, in Area Science Park, 34012 Trieste, Italy*
[4]*Physics Department, University of Trieste, via A. Valerio 2, 34127 Trieste, Italy*
[5]*Laboratorio Tecnologie Avanzate Superfici e Catalisi, Istituto Nazionale per la Fisica della Materia, Padriciano 99, 34012 Trieste, Italy*
[6]*International Centre for Theoretical Physics (ICTP), P.O. Box 586, 34014 Trieste, Italy*

(Received 12 April 2001; published 11 October 2001)

We show that a fluctuating incommensurate domain wall structure such as that hypothesized for clean Ge(111) above 540 K and the observed weakly metallic behavior can be mutually related in an unexpected manner. The wall structure implies a liquid of defects—adatom trimers at the intersection of three concurrent topological walls—that carry fractional charge, one half extra electron each. These electrons are delocalized among defects, giving rise to a narrow band 2D metal, whose Fermi level density of states grows with the density of walls and thus with temperature. This model agrees strikingly with new photoemission measurements carried out on Ge(111) across the 540 K transition and beyond.

DOI: 10.1103/PhysRevLett.87.186802 PACS numbers: 73.20.–r, 73.25.+i, 73.90.+f

Topological defects [1] carrying fractional charge [2] have played an important role in solid state physics, thanks to very transparent and popular examples such as solitons in 1D polyacetylene chains. The role of topological defects is to act as boundaries between degenerate ground states. This Letter describes an unusual point defect in two dimensions, which may arise, for example, on certain semiconductor surfaces. While not a conventional topological defect in the usual sense, the new defect arises as the intersection of three topological line defects, or walls. Remarkably, the walls are neutral, but the defect carries fractional charge, precisely half an electron. The impossibility to localize half an electron requires these two-dimensional electrons to remain itinerant, so as to be shared by at least two defects over arbitrarily large distances. We shall present theoretical and experimental evidence suggesting that the weak metallic behavior displayed above 540 K by clean Ge(111)—certainly one of the best characterized and documented systems in surface science [3–12]—could have precisely this origin.

The stable state of clean Ge(111) at room temperature is a $c(2 \times 8)$ reconstruction, consisting of a well-ordered quarter of monolayer of Ge adatoms [3]. Each Ge adatom occupies a T_4 site and saturates three of the four ideal (111) surface dangling bonds in the cells. The adatom's fourth valence electron is effectively transferred to the unsaturated surface ("rest") atom [4], yielding a passivated, insulating surface, stable up to $T_s \simeq 540$ K. Here the surface transforms, with a first order reversible transition, to a disordered state. STM has shown that liquidlike adatom mobility occurs in this state [5]. Electron diffraction [6–8] shows the sudden replacement of fourth order spots by weak incommensurately split half-order reflections. The splitting δq jumps from zero to a finite value of 0.17 Å^{-1} at T_s and then increases continuously with temperature. A weak metallic surface conductivity growing with $T > T_s$ roughly paralleling δq was found by inelastic electron spectroscopy [9] but no quantitative connection was drawn thus far between the various phenomena.

The STM picture of a 2D liquid represents a long-time average, perfectly compatible with some instantaneous form of incommensurate order, only slowly fluctuating through relatively rare diffusion events. As far as the electronic structure is concerned, this slow diffusion is irrelevant, and we can concentrate on the instantaneous structure. A plausible structural explanation of the incommensurate phase is provided by the Phaneuf-Webb (PW) model [7]. In that model, the Ge adatoms persist above T_s, but they abandon the $c(2 \times 8)$ periodicity to give rise to large (2×2) domains separated by a quasihexagonal network of antiphase domain walls (Fig. 1a). The walls possess a local $c(4 \times 2)$ structure, so that the PW model is simply related to the parent $c(2 \times 8)$ phase [made of minimally wide parallel (2×2) and $c(4 \times 2)$ stripes] by expansion of the (2×2) area from stripes to isotropic domains. No expansion occurs for the $c(4 \times 2)$ stripes, which make up the incommensurate domain walls between adjacent (2×2) domains. Besides a wealth of indirect spectroscopic evidence [10,11], this model is directly supported by STM evidence on Ga-rich Ge(111) [13], where the role of Ga is to freeze out the adatom diffusion. Further STM studies [14] show that on that surface, slow adatom ring exchange processes take place at room temperature to displace the walls and correspondingly expand/contract the (2×2) domains, exactly as hypothesized by Phaneuf and Webb.

In the PW model, the walls between (2×2) domains possess a clear topological character. The (2×2) phase

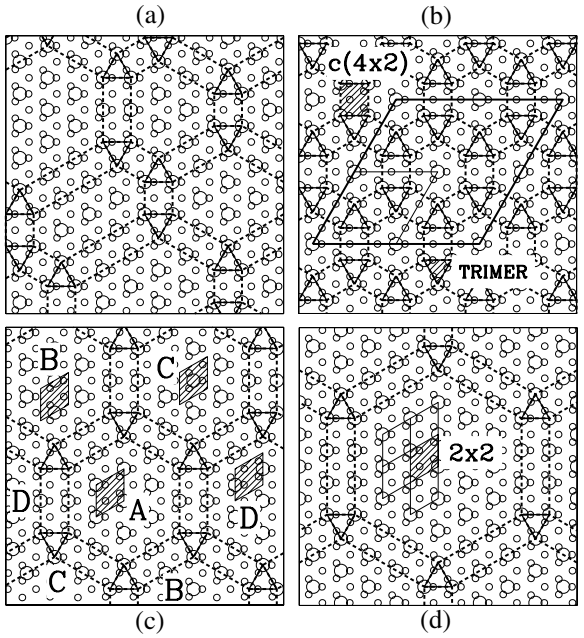

FIG. 1. The Phaneuf-Webb model [7]: (a) a sample incommensurate pattern; (b)–(d) the three regular patterns used in our calculations ($N = 6, 18, 36$). In (c) the four 2×2 "colors" A, B, C, and D are indicated. Triangles mark the trimer defects.

inside the domain is fourfold degenerate, with four "colors" A, B, C, and D. Symmetry implies [1] the existence of $\binom{4}{2} = 6$ distinct topological line defects — walls — separating two colors. The topological nature of the walls is best appreciated by assuming a regular hexagonal packing of (2×2) domains, as in Figs. 1b–1d. Here the true, physical unit cell (small rhombus) falls short of joining identical colors at the boundaries, as one might perhaps have expected a unit cell to do. It takes a doubling of cell size in both directions to do that. But doubling is redundant, as the system is genuinely invariant against the shorter translations that make up the small rhombic cell. The color phase shift at the small cell boundary is compensated inside the cell by the wall defects that are thus topological. The walls here consist of $c(4 \times 2)$ stripes, where the 2D adatom density (coverage) is $1/4$, exactly as inside the 2×2 domain. They are therefore *neutral,* carrying neither extra adatoms nor extra charge. Nonetheless the PW model, which is an array of walls, does contain excess adatoms compared to the $1/4$ coverage of the commensurate surface. That excess is entirely restricted to the zero-dimensional defect regions where any three walls concur. The defect is an adatom triangle or trimer, also describable as half a $(\sqrt{3} \times \sqrt{3})$ cell. Here adatoms are denser, corresponding to a local coverage of $(1/3)$. The PW model can thus be seen as a liquid of these trimer defects. They are not topological in a conventional sense, as the order parameter symmetry does not allow for irreducible point defects. However, they do arise as the by-product of topological walls, and as we shall see, they also possess remarkable properties such as fractional charge.

A characterization of the electronic properties of the trimer defects starts with adatom and electron counting. Using the regular PW model of Figs. 1b–1d as a working example, $4N + 3$ is the number of first layer atoms in the cell, and $N + 1$ is the number of adatoms, so that the coverage is a factor $(N + 1)/(N + 3/4)$ higher than the insulating $1/4$ coverage of the (2×2), $c(4 \times 2)$, or $c(2 \times 8)$ commensurate structures. With $N + 1$ adatoms and N rest atoms in the cell, the excess adatom contributes its single unpaired p_z electron to surface states, which must therefore become partly filled and metallic. Each trimer defect contains exactly $1/2$ excess adatoms, so that it takes *two* defects in the cell to jointly make up for one extra adatom and extra electron. None of them separately does, in spite of the fact that their spatial separation may be very large. Charge fractionalization, usually the hallmark of topological point defects [2], emerges at this less conventional defect too. Here the electron itself is fractionalized, and quantum mechanics requires an impossibility for the wave functions to localize on a single defect. In other words no matter how far two "partner" trimer defects — defined as the two closest trimers at the two end points of the same wall segment — might be, the defect-induced electronic states must be extended so as to share the electron state. While this requirement is of additional interest in the presence of disorder, we will examine the simple regular case first. In order to exemplify with a lattice of trimer defects, we carried out tight binding calculations for a set of regular periodic PW model surfaces.

As in Figs. 1b–1d, we took (2×2) hexagonal domains of increasing size, corresponding to cell sides of increasing lengths $L = 20.8$, 34.7, and 48.6 Å. The precise positions of atoms within each cell were set by periodically repeating the equilibrium surface geometry obtained through a plane wave calculation of a single 2×2 Ge(111) cell [15]. All cells consisted of slabs three bilayers thick, with $N + 1$ adatoms at T_4 sites and with the bottom surface saturated with $4N + 3$ hydrogen atoms. The three cells considered, $N = 6$, 18, and 36, contained $N_T = 25N + 19 = 169$, 469, and 919 Ge atoms, of which $N + 1 = 7$, 19, and 37 are adatoms. The corresponding coverages are $7/27$, $19/75$, and $37/147$, all slightly larger than $1/4$. There are in each case two trimer defects per cell, each contributing one half extra adatom, and thus one half conduction electron. The cell sizes L of our systems are related to a theoretical splitting of half-order LEED spots, δq, through the relation $L = 2\pi/\delta q$. By identifying this splitting with the measured one, we can associate a temperature to each of our three model cell sizes. The smallest cell, with $L = 20.8$ Å, corresponds to $T \simeq 800$ K; the medium-sized cell, with $L = 34.7$ Å, to $T \simeq 600$ K; for the largest cell, with $L = 48.6$ Å, δq is smaller than that observed at $T_s \simeq 540$ K. These regular cells are, of course, strongly idealized, when compared with the generally irregular and fluctuating geometry expected in the real system.

Electronic states were calculated by empirical tight binding. First neighbor interaction parameters were chosen by

fitting the calculated tight binding electron bands to those obtained by a plane wave calculation for two smaller systems, namely, a 2×2 and a $\sqrt{3} \times \sqrt{3}$ Ge(111) cell. The calculation yields a large overall number $4N_T + 4N + 3 = 104N + 79$ of bands (not shown). Of these, $2N_T + N + 1$ are filled valencelike bands well below E_F, and an equal number are empty conductionlike bands well above E_F. Of the remaining $2N + 1$ states, N are filled rest-atom states slightly below E_F, and $N + 1$ nonbonding bands are grouped at midgap, right across E_F. In Fig. 2, the midgap group of bands is shown for the smallest PW cell. In analogy with earlier calculations of 2×2 and $\sqrt{3} \times \sqrt{3}$ surfaces [15], we identify these surface states as 2D adatom dangling bond bands, lying inside the band gap surface of the otherwise insulating 1/4 covered surface. The total valence electron number is $4N_T + 4N + 3$ so that after filling all the valence bands and the rest-atom states, there is just one more electron per cell left. Thus, the lowest of the midgap surface bands is exactly half filled, explaining the weak metallic character for these surfaces. We also see that the density of occupied states decreases as the cell size increases. Since increasing cells correspond to a decreasing incommensurate splitting and thus in experiment to a decreasing temperature, we conclude that the surface metallicity should increase with temperature. We computed the electronic density of states (DOS) at the Fermi energy, $n(E_F)$ (Fig. 2b), and found about 6.0, 4.3, and 3.0 states/(eV $\times$ adatom $\times$ spin) for the small, medium, and large cells, respectively.

To bring out the signature of the trimer defects as the fractional donor states, we analyzed the wave function amplitudes at the Fermi energy. The tight binding model allows us to compute the square amplitude of every given state on every given atom. A maplike plot of the state at E_F is shown in Fig. 3. It reveals indeed a large amplitude at the trimer defects, but also *on the whole wall network that joins the defects*. That is at first sight surprising, because metallic electrons are donated by the trimers alone, the walls being neutral. However, the trimers act as very atypical donors. The contributed extra half electron is pushed out from the trimer, and distributed uniformly on the wall segment connecting with other trimers, instead of piling up nearby, as one could have expected for a standard integer-electron donor. This atypical behavior provides an indirect but clear clue about the charge fractionalization in the defect. The latter implies a necessity of wave function delocalization between defects, which is absent for ordinary, integer donors. While more accurate calculations including the Coulomb attraction between the partly ionized defect adatoms and the delocalized electrons, electron-electron repulsion, and disorder are needed to make this aspect more quantitative for possible experimental detection, the total delocalization of electrons donated by trimer defects pinpoints them as fractional electron donors.

The above theoretical findings have a direct experimental counterpart. Electron energy loss (EEL) [9] showed earlier on that the $c(2 \times 8)$-incommensurate phase transition is accompanied by a surface semiconductor-metal transition. It was suggested that the weak metallicity of the incommensurate phase could have a common origin with the theoretically calculated backflow of electrons following the adatom diffusion [9,12]. In fact, both phenomena depend on the presence of unsaturated, metallic surface states. In order to focus on the metallic Fermi level DOS in the incommensurate phase just calculated, we performed high resolution photoemission for the Ge(111) surface

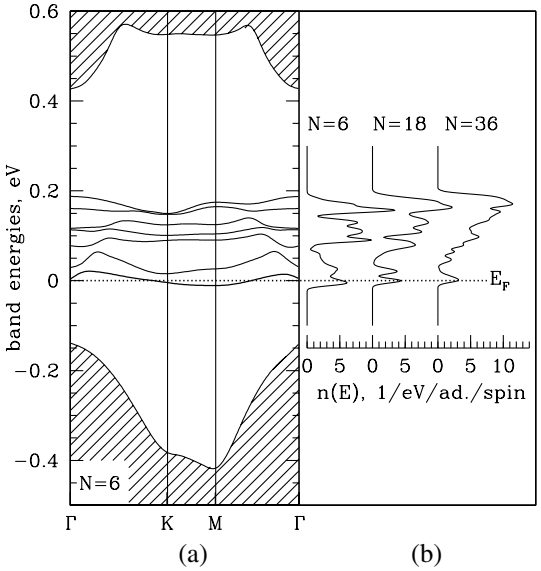

FIG. 2. (a) Calculated surface bands ($N = 6$); (b) density of states ($N = 6, 18, 36$).

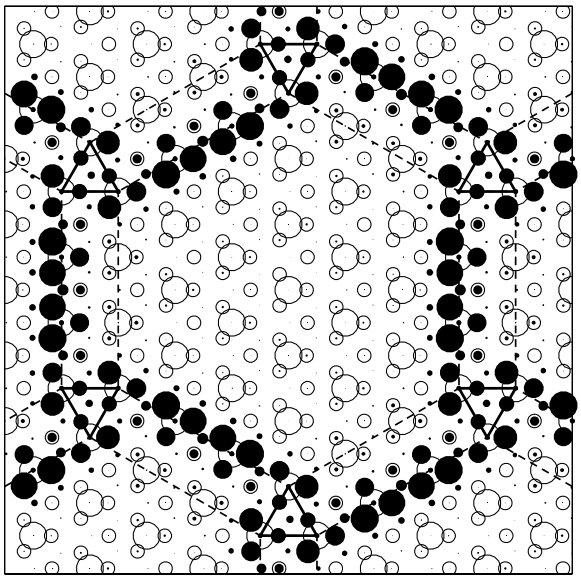

FIG. 3. Calculated electron density map ($N = 36$) for the half filled surface band at point K. Large black circles indicate large values. The lack of propensity to localize on individual trimer defects is a consequence of fractionalization.

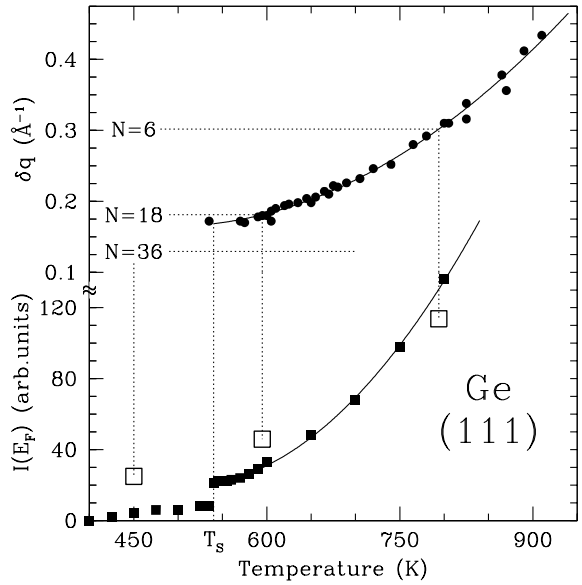

FIG. 4. Top: δq as a function of T (from Ref. [7]): the values for our model cells are shown. Bottom: theoretical (large open squares) and experimental (full squares) electron spectral intensity at E_F.

between RT and 800 K, by using He I radiation ($h\nu = 21.2$ eV) and collecting spectra at 12° relative to the surface normal along the Γ-M direction. The overall energy resolution was 55 meV. Details about sample preparation and measurement setup have been reported elsewhere [10]. The sample temperature was measured by means of a thermocouple glued on the back side of the wafer, with a maximum error of ± 3 K.

The photoemission valence band spectra of Ge(111)-$c(2 \times 8)$ in the energy region near E_F are characterized by two features at about 0.7 and 1.4 eV [10,11], due to the rest atom p_z dangling bonds, and the back bonds, respectively. They provide a fingerprint of adatom-rest-atom pairs at the Ge(111) surface. These features remain visible well above T_s, confirming survival of adatom-rest atom in the incommensurate phase [10,11].

We presently measured the photoemission spectral intensity at E_F shown as a function of temperature on Fig. 4. At 300 K the chemical potential is pinned about 0.1 eV above the valence band (and surface band) top, independent of temperature [10]. Analyses of the core level [10] and of the surface states [10,11] indicate a shift of less than 10 meV between 300 and 800 K, while the surface gap decreases from 0.55 eV at 300 K to 0.22 eV at 700 K. Thus, the chemical potential remains in the surface gap in this interval. The spectral intensity at E_F is negligible from 300 up to 400 K, where it starts to increase with temperature, remaining very weak up to $T_s = 540 \pm 3$ K. At 540 K there is a sudden upward intensity jump of about 120% within about 3 K, followed by a further continuous temperature-driven increase. The upward jump of spectral intensity at T_s indicates the onset of metallicity at the incommensurate transition, first detected by EELS [9]. It confirms a first order transition, as do the structural data. The jump cannot be attributed to thermally excited carriers across the surface adatom-rest-atom gap, which is found by EELS [16] to take values fit by 0.6 eV—(0.0005 eV/K)T (no jumps) up to 700 K. Thermal excitation across that gap could at most account for the much weaker spectral intensity seen below T_s. We instead identify the observed spectral density at E_F with the metallic density of states, just calculated and related through the PW model to the temperature-dependent incommensurability. To check that, we extracted from the temperature dependence of the peak splitting of the half-order LEED spots [7] the mean domain size. It decreases linearly with temperature as $L_0 - m(T - T_s)$, where L_0 and m are the mean size at T_s and rate of decrease, respectively [13]. Using that, we compared in Fig. 4 the measured and calculated spectral intensities at E_F, to find them in fairly good agreement which, in view of the crudeness of the model, is rather gratifying.

We conclude that the weakly metallic surface conduction electrons detected in photoemission on clean incommensurate Ge(111) most likely originate from self-doping by the trimer defects. The fractional nature of that doping should reflect in a peculiar electron delocalization. Even though further progress must await a proper treatment of disorder and correlations, which should be quite interesting in this model, it seems likely that the relatively high conductivity observed at very reduced 2D electron densities should not be unrelated to that delocalization.

This work was supported through MURST COFIN 99 and INFM Calcolo Parallelo.

[1] G. Toulouse and M. Kleman, J. Phys. (Paris) Lett. **37**, L149 (1976).
[2] R. Jackiw and J. R. Schrieffer, Nucl. Phys. **B190**, 253 (1981).
[3] R. S. Becker *et al.,* Phys. Rev. Lett. **54**, 2678 (1985).
[4] R. D. Meade and D. Vanderbilt, Phys. Rev. B **40**, 3905 (1989).
[5] R. M. Feenstra *et al.,* Phys. Rev. Lett. **66**, 3257 (1991).
[6] T. Ichikawa and S. Ino, Solid State Commun. **34**, 349 (1980).
[7] R. J. Phaneuf and M. B. Webb, Surf. Sci. **164**, 167 (1985).
[8] J. S. Ha and E. F. Greene, J. Chem. Phys. **91**, 7957 (1989).
[9] S. Modesti *et al.,* Phys. Rev. Lett. **73**, 1951 (1994).
[10] A. Goldoni *et al.,* Surf. Sci. **382**, 336 (1997).
[11] T. Yokotsuka *et al.,* Jpn. J. Appl. Phys. **23**, L69 (1984).
[12] N. Takeuchi, A. Selloni, and E. Tosatti, Phys. Rev. Lett. **69**, 648 (1992).
[13] P. Molinas-Mata and J. Zegenhagen, Phys. Rev. B **47**, 10 319 (1993).
[14] Z. Gai *et al.,* Phys. Rev. B **53**, 13 547 (1996).
[15] G. Ballabio, S. Scandolo, and E. Tosatti, Phys. Rev. B **61**, 13 345 (2000).
[16] A. Goldoni *et al.* (unpublished).